We supply below a full response to the reviewers' comments. A version of the revised manuscript, with changes tracked, is appended.

REVIEWER #1.

The paper presents a targeted model study on the evaporative shrinking of diesel particles over timescales representative for the dispersion on the neighbourhood scale. The model study explores the sensitivity of nucleation-mode diesel particles to the volatility of the initial chemical composition represented by a mixture of surrogate molecules, the higher n-alkanes, in a very systematic manner. Gaussian distributions of the n-alkanes with carbon numbers between 16 and 32 with various bandwidths are systematically tested for three different vapour pressure datasets. The influence of a non-volatile core with various mass fraction in the nucleation mode is also tested. A new concept of threshold modal composition is introduced which allows identification of the components for which an accurate vapour pressure estimation is most critical. The paper is well written for the most part and results are presented in a structured way. Input datasets and model results of the study are well documented and easily accessible.

Answer: we thank the referee for their assessment of the scope and importance of the manuscript.

It is claimed that the method has the potential to improve the efficiency of urban aerosol models. I had expected to see a comparison of the suggested simplifications with the full model and an estimate of the computational savings.

Answer: such a comparison is beyond the scope of the paper. We have removed the final sentence in the abstract.

The main problem is that the analysis was restricted to the process of condensation/evaporation alone.

Answer: CiTTyCAT UFP contains treatments of coagulation, deposition, and exchange with the free atmosphere. Our earlier work (Nikolova et al., 2016, Faraday Discuss.,189, 529-546, DOI: 10.1039/C5FD00164A) has shown that deposition and coagulation have a minor effect in the current scenario and so were switched off to allow a more straightforward diagnosis of model behaviour. We have amended the revised ms at line 208-210 of the version with tracked changes (see manuscript version appended) to say: "Our earlier work (Nikolova et al., 2016) has shown that deposition and coagulation have a minor effect in the current scenario and so were switched off to allow a more straightforward diagnosis of model behaviour."

Specific Comments

1.) The exhaust size distribution from laboratory test-rig measurements (Figure 2-S) shows a broad distribution of n-alkanes in the diameter range < 10-18 nm with a maximum at C29H60 and a range of +/-7 corresponding to sigma = 3. In contrast, most realisations of the current model setup resulted in solutions with a narrow distribution of n-alkanes with carbon number < 18 (this includes all solutions for vapour pressure datasets A-a and B-c) to explain the REPARTEE-like behaviour. These n-alkanes are predominantly in the gas-phase under ambient atmospheric conditions. Only for vapour pressure dataset B-c, which has the highest vapour pressure for all n-alkanes, the model gives solutions with carbon number > 20 and broad distributions (sigma = 3 to 5) for the REPARTEE-like behaviour (P.15, lines 372-373). It looks like other processes, consistent with an initial nucleation mode composition of higher-carbon-number compounds, are relevant.

Answer: In this study we propose a systematic method to evaluate the evaporative potential of nucleation mode particles (diameter less than 30 nm) of varying composition under ambient conditions. Our approach is to 'scan' the available compositions efficiently using the 'mode composition plus sigma' method we describe, and then — subsequently — to compare model

outcomes to the field observations and the laboratory measurements. That is, we do not assume a priori that any given vapour pressure set or composition is correct. We do not need any other aerosol processes in the model to find compositions that are consistent with the field observations and lab experiments.

2.) Coagulation was obviously not included in the model setup (P.8, line 192). Coagulation is enhanced through the shrinking of particles by evaporation (Jacobson et al.,2005). As particles shrink, their coagulation rates with larger particles will increase.
Although evaporation has a greater effect on the evolution on the particle size distribution in the first second, coagulation will become more important towards longer time scales and may be dominant at 100 s. When evaporation and coagulation are treated together, there will be a feedback of coagulation on the composition of nucleation mode particles. This is because coagulation affects the vapour pressures of n-alkanes in particles of a given size through the Raoult's Law. This feedback may well influence the calculated nucleation mode peak diameter.
Answer: Coagulation was not included in the model setup for this scenario, as discussed above. Our coagulation tests used the same model and so included the size-dependence of coagulation rates. Text amended as described above.

3.) P.5, lines 114-116: The range of volatility of the particle composition in the diesel exhaust emissions is not known. However, formation of a volatile nucleation mode is evident in a laboratory system that mimics real-world dilution of diesel exhaust (Arnold et al., 2012; Rönkkö et al., 2013). Aerosol dynamics models show that low volatile and extremely low volatile organic compounds are required to explain the evolution of the volatile nucleation mode during cooling and expansion of the exhaust (Rönkkö et al.,2013; Pirjola et al., 2015).
Answer: Our study does not consider the cooling and expansion of the exhaust plume. Instead, we have examined the evaporative potential of particles under ambient conditions, timescales ~100 s, distances 10 m - 1 km and size distribution that is typically observed in proximity to traffic sites (Nucleation mode Dp = 23-25 nm, Aitken mode Dp at around 50-60 nm, Dal'Osto et al 2011). The REPARTEE-like behaviour could only be explained if low-carbon-number compounds are present in the particle. However, the evaporation is dependent on the vapour pressure and we show in Figure 6-S the relative differences in the nucleation mode peak diameter using B-c (highest vapour pressure values) and A-a (lowest vapour pressure values). Overall, the largest differences in the 100-s Dpg,nuc occur for modal compositions between C22H46 and C24H50 and composition standard deviation from 1 to 3. i.e., the range where the highest relative differences occur is not in the low-volatile nor extremely-low volatile organic compounds. We have amended the text at line 138-139 to remind the reader that the simulation is focused on events after dilution and cooling, in section Introduction, as follows: 'The model simulations are focused on events after dilution and cooling of the exhaust-pipe plume.'

4.) P.8, line 184: A higher number of bins representing the small particles would give a more accurate result for the relevant part of the size distribution. How does a larger number of size bins, for instance 25, change the result on the REPARTEE-like behaviour?
Answer: In our study we use 15 size bins, 6 of which are located in the nucleation mode. This provides sufficient details in the nucleation mode and a reasonable amount of size bins, attractive for implementation in large 3-D models. We cannot see a reason in the physics for a substantive change in our results when running with more bin resolution.

5.) P.9, line 197: how fast is the dilution in the first second? Preferably, the dilution ratio of the modelled total particle number after 1 s should be given and compared to literature data.

Answer: The model simulations are focused on events after tailpipe dilution and cooling. Dilution has been considered for gas-phase concentration of the participating compounds in the box. Background gas-phase concentration is kept at zero. This information is now added in lines 281-282.

6.) P.11, line 251: Gas-phase n-alkanes C16H34 and C17H36 can be oxidized by the OH radical leading to oxygenated products with lower vapour pressures (Jordan et al., 2008). An estimate should be given how much gas-phase oxidation can affect the modelled size distribution on the time scale of 100 s.
Answer: The rate coefficient of C16H34 according to Atkinson and Array (2003) is 23.2×10^{-12} cm^3 $molec^{-1}$ s^{-1}. The hydroxyl (OH) radical concentration is typically around 10^6 molec cm^{-3}. Hence the timescale for oxidation of C16H34 is about 10^6 s, a time much larger than the 100 s considered in this study. We add at line 279-281: "For hydroxyl (OH) radical concentration ~10^6 molec cm^{-3}, the timescale for oxidation of $C_{16}H_{34}$ is about 10^6 s (Atkinson and Arey, 2003). Therefore oxidation of SVOC is neglected given the timescale in our study (100 s)."

7.) P.17, lines 409-410. Which assumptions were made regarding the mixing with the non-volatile core? If the non-volatile component is able to influence the gas-particle partitioning, for example due to its absorptive nature, then the evaporation rate will be affected by a decrease of the vapour pressure of the volatile compounds in the mixture through the Raoult's Law. If the non-volatile core is not in a mixture with the n-alkanes, there is no Raoult's Law depression of the vapour pressure of the volatile compound. The assumption about the non-volatile core will also affect the conclusion about its chemical composition in the nucleation mode (organic carbon or lubricant oil metal compounds).
Answer: In this study, the non-volatile component is not considered as part of the mixture, therefore does not affect the saturation vapour pressure of the volatile compounds. The activity coefficient in our study is assumed to be unity in the absence of any additional information about the ideality of the solution. In-particle-phase processes and in-particle chemistry are not considered. The referee is correct to point out the difference effects that organic carbon and metal compounds will have on SVOC vapour pressures and we have corrected the ms so that it now reads at line 208-210: "The condensation/evaporation process applies Raoult's Law (for an ideal solution of the volatile compounds) and a mass accommodation coefficient $\alpha = 1$ (Julin et al., 2014) for all SVOC"

Technical Corrections
Abstract p.3, line 52-54. Mention the uncertainty range of the vapour pressures for n-alkanes between C22H46 and C24H50 based on the vapour pressure datasets displayed in Figure 3.
Answer: We have added information on the uncertainty range as suggested as follows (lines 260-261): 'The vapour pressure ranges of $C_{22}H_{46}$ and $C_{24}H_{50}$ are between [9.23×10^{-3} and 8.94×10^{-6} Pa] and [2.26×10^{-3} and 2.46×10^{-7} Pa], respectively.'

P.4, line 71: Add information on size range.
Answer: Information on the size is added at line 76ff, as follows: 'Harrison et al. (2011) reported that on a busy highway in central London, UK, 71.9% of particles by number were traffic-generated; of which 27.4% are found in the semi-volatile exhaust nucleation mode (size between 15 and 30 nm), 38% are in the exhaust solid mode (size > 30 nm) and the remaining 6.5% are from brake dust and resuspension (size > 2000 nm).

P.4, line 79: Jacobson et al. (2005) and Karl et al. (2016) should be included in this list.
Answer: The references are included at lines 82ff, as follows: 'Experimental and modelling studies have advanced our understanding of the behaviour of urban air UFP, e.g. the relevant aerosol dynamics important to the evolution of the UFP in space and time (Jacobson, 2005; Allen et al., 2007; Biswas et al., 2007; Dall'Osto et al., 2011; Nikolova et al., 2011; Karnezi et al, 2014, Karl et al., 2016).'

P.7, line 168: missing ", respectively" at end of this line.
Answer: Done.

P.10, line 227-232 and Figure 3: the vapour pressure data from Lemmon and Goodwin(2000) should be included in Figure 3 to facilitate comparison with previous studies on the volatility of exhaust particles near roadways (Zhang and Wexler, 2004; Zhang et al., 2004; Karl et al., 2016).
Answer: Figure 3 and caption are now updated with Lemmon and Goodwind (2000) vapour pressure, which has a range of vapour pressure is very similar to Compernolle et al. (2011). Also, we have added the reference in the description of vapour pressures parameterisations in section 2.3 at line 250, as follows: ' Figure 3 shows vapour pressures above pure, flat, supercooled liquids for n-alkanes in the range C16H34-C32H66, following Chickos and Lipkind (2008), Compernolle et al. (2011), Lemmon and Goodwin (2000), the Epi Suite calculator (US EPA, 2017), and the UmanSysProp tool (Topping et al., 2016).'

P.10, line 237: A-a is mentioned before it is defined in the text.
Answer: The text, now at line 261ff, reads: 'An enormous difference in the vapour pressure for C32H66 (from 2.66x10-5 Pa in Epi Suite, to 3.20x10-15 Pa in Nannoolal et al., 2008 with the boiling point of Joback and Reid, 1987, called A-a hereafter) is clearly seen in Figure 3.'
…and at lines 267ff: ' For the purpose of our sensitivity study, three representative datasets are nominated as input, namely: Myrdal-Yalkowsky (1997) with the boiling point of Nannoolal et al. (2004, called B-c in Figure 3 and hereafter); Compernolle et al. (2011, called Co); and A-a.'

P.11, line 270: Please add the abbreviation (Co) for this vapour pressure dataset here.
Answer: Done.

P.12, line 291: Here the concept of threshold modal composition is introduced for the first time. It would be good to add a paragraph on the reasoning behind this concept.
Answer: We have expanded our description at lines 318ff, as follows: 'For a modal composition of $C_{21}H_{44}$, increasing σ makes almost no difference to the model outcome at 1 s. Below, we call the modal composition that shows insensitivity to σ for a given model output time, the *threshold modal composition*. The threshold modal composition points to the composition compound that is in equilibrium between gas and particulate phases for the selected timescale. Lower-carbon-number compositions than the threshold modal composition evaporate quicker and therefore have reached equilibrium with their respective gas concentrations on a much shorter timescale. The higher-carbon-number compositions evaporate slowly and are out-of-equilibrium with their respective gas concentrations for the selected timescale.'

P.15, line 358: Although the model results with the vapour pressure dataset Co are explained in detail in section 3.1, it would help the reader to give a short summary of Co results regarding the REPARTEE-like behaviour before A-a and B-c results are discussed.
Answer: We have added the following (lines 385-387) 'Diameter change when using Co vapour pressure has been discussed in the previous section. The values of vapour pressure in the Co data are intermediate between the B-c and A-a data. Hence, $D_{pg,nuc}$ at 100 s using vapour pressure parameterisations A-a and B-c (see Supplementary Information), as expected, shows the same general behaviour as for vapour pressure parameterisation Co, but with a marked change in threshold modal composition.'

P.19, lines 472-477. There seems to be something wrong with the logic of the two sentences. The second sentence contradicts with the statement on p.30, lines 492-493.
Answer: We thank the reviewer for spotting this discrepancy. The word greater is replaced with the word lower to comply with the logic of the statements as follows at lines 517ff: 'For components with volatility less than that for the $C_{22}H_{46}$ surrogate compound used here, all available vapour pressure parameterisations render these compounds volatile over the 100-s timescale. These components will equilibrate with the gas phase on these short timescales. Components with volatility **lower** than that of the $C_{24}H_{50}$ surrogate are effectively non-volatile over this timescale for all vapour pressure parameterisations, and so will remain condensed and out-of-equilibrium with the gas phase on these timescales.'

Figure 1: Contours of the GCxGC chromatogram are hardly visible due to the overlay with the coloured polygons. For clarity, it would be better to show the original chromatogram beneath the current figure plot. Annotate x-axis and y-axis of the upper bar charts
Answer: The coloured polygons in this Figure illustrate that the carbon number distribution does not increase in the same way for different homologous series with increasing retention time (volatility). For example, a C15-alkane has the same volatility as C14 monocyclic alkanes, C13 aldhydes and ketones and C14 monocyclic aromatics. Removing these polygons will not demonstrate this point and the original chromatogram without the polygons will be less informative than is presented in this figure. The polygons provide quick view of the volatility (y-axis) in the homologous series. The contour plot provides the peak intensity and not the mass concentration on the chromatogram. The bar chart on top indicates the total alkane and total mass concentrations per volatility bin, where the x-axis is retention time like what is labelled in Figure 1. The y-axis is percentage mass concentration, which has been added to the Figure.

REVIEWER #2.
This reviewer cannot agree with the shrinkage of diesel particles in urban air undergoing evaporative when advected to a cleaner atmosphere, as presented in this study and those reference papers cited. The reviewer also has no solid reason to reject the hypothesis. Supposed that the hypothesis is correct, the modeling results delivered in this study are valuable for research community.
Answer: we thank the reviewer for their open-minded reading of our ms.

Two issues might be helpful for potential readers: 1) the temperature change in the initial few second dilution and how this affects particle number size distribution;

Answer: Please see the discussion of review #1 above. We do not consider expanding and cooling exhaust plumes, but rather study the neighbourhood-scale transport of the diluted exhaust. We have amended the text at line 138-139 to remind the reader that the simulation is focused on events after dilution and cooling.

2) How does the Kevin effect affect the hypothesized evaporation?
Answer: This information is added in section 2.1 (lines 213ff) as follows:
'The Kelvin effect is also considered, which alters the saturation vapour pressure of the compounds as a function of the particle diameter, the surface tension of the SVOC mixture/solution, and the molecular weight of the participating compounds. The Kelvin effect is pronounced for particles with a diameter less than 20 nm and substantial for particles with diameter less than 10 nm. The Kelvin term accelerates the evaporation for all compounds under consideration in this study and more notably for the high-molecular-weight compounds due to their larger molar volume.'

REVIEWER #3.

Nikolova et al. have used a numerical model to simulate the evaporation of ultrafine particles (UFP) from diesel exhaust under a range of input conditions and have used the model results to develop insight into the organic composition of these UFPs. By informing their model with inputs based on field measurements, they find that certain combinations of model inputs (e.g., <5% of the UFP material can be treated as a nonvolatile core) are able to reproduce the observed change in the mode of these UFPs. The motivation for this study is clear and the results are presented in a clear and consistent manner. However, there are several deficiencies in the description of the methods and possibly also in the processes the authors may not have included in their model.
Answer: we thank the reviewer for their comments of our ms.

In my view, the authors have undertaken a rather narrow study but need to expand it if they are too truly probe the variable space that can help explain the observations. At this point, I do not recommend publication in ACP until the authors have had a chance to review and respond to my comments.
Answer: We believe that our study is of sufficient depth and general interest to warrant publication, and is further enhanced by our answers to the comments below.

Major comments: 1. Organic species distribution: The authors have assumed a Gaussian distribution to model the organic species distribution. Is it possible that the distribution is bimodal? Also, there are plenty of volatility distribution data for diesel exhaust that could be used to inform the type of distribution (e.g., Gaussian) as well as the spread of the distribution (e.g., standard deviation>X); e.g., Robinson et al. (2007), Grieshop et al. (2009), May et al. (2013). These data could also be used to eliminate certain input choices.
Answer: We thank the reviewer for pointing to the references. Recall that our strategy is to scan the vapour pressure and composition distribution and — subsequently — compare with field and laboratory studies. We agree that those studies show a Gaussian-type distribution centred at volatile SVOC with quite wide standard deviations. Therefore, we have included these references in our discussion as follows (lines 501ff): 'The work of Robinson et al. (2007), Grishop et al. (2009) and May et al. (2013) also point to a Gaussian-type distribution of the exhaust particle composition centred at SVOCs, that has a wide standard deviation.'
Our strategy takes a Gaussian approach to the definition of the composition. We cannot, therefore, rule out multi-modal or other distributions that differ strongly from a Gaussian. We have drawn the reader's attention to this limitation of our study at line 182ff: 'Multi-modal compositions, or others differing strongly from Gaussian, are not investigated in the present study, but could be

accommodated by a simple extension of the method.'

2. Model details: Several aspects of the model framework are unclear since they are not reported in the main text. Does the model simulate coagulation and nucleation? If yes, how is it dealt with? There is plenty of evidence, particularly with secondary organic aerosol systems, that diffusion limitations in the condensed phase could extend evaporation timescales and the time required for semi-volatile material to reach equilibrium as well as change the dynamics of how an aerosol size distribution evolves over time (e.g., Shiraiwa and Seinfeld (2012), Zaveri et al. (2017)). Is this modeled here? If not, this would be an important process to include. Is the Kelvin effect considered? If yes, how is it modeled? If not, why is not modeled? How does dilution affect the results? Could dilution be modeled to examine the sensitivity in the findings? I have not read the original measurement papers but were there any tracers (e.g., CO) that could be used to account for dilution of the Lagrangian box?

Answer: This study does not consider coagulation and the information is now added in lines 208ff : 'Our earlier work (Nikolova et al., 2016) has shown that deposition and coagulation have a minor effect in the current scenario and so were switched off to allow a more straightforward diagnosis of model behaviour.'

Nucleation is not considered because the model simulations are focused on events after dilution and cooling (lines 138ff). Secondary organic aerosol formation and oxidation of SVOC are neglected due to the large timescale in comparison to the timescale in our study. This is now explained in lines 279ff as follows: 'For hydroxyl (OH) radical concentration ~10^6 molec cm^{-3}, the timescale for atmospheric oxidation of $C_{16}H_{34}$ is about 10^6 s (Atkinson and Arey, 2003). Therefore oxidation of SVOC is neglected given the timescale in our study (100 s).'

The model considers the Kelvin effect. This is explained now in lines 213ff: 'The Kelvin effect is also considered, which alters the saturation vapour pressure of the compounds as a function of the particle diameter, the surface tension of the SVOC mixture/solution, and the molecular weight of the participating compounds. The Kelvin effect is pronounced for particles with a diameter less than 20 nm and substantial for particles with diameter less than 10 nm. The Kelvin term accelerates the evaporation for all compounds under consideration in this study and more notably for the high-molecular-weight compounds due to their larger molar volume.'

Dilution has been considered for gas-phase concentration of the participating compounds in the box whereas background gas-phase concentration is kept zero (lines 281-2).

3. Model inputs: Similar to details about the model framework, certain aspects about the model inputs are unclear too. Is the same organic species distribution assumed for all particle sizes? What is the rationale for that? Do the model results change if the organic species distributions are size dependent? Related to the size-resolved composition question, is it also important to consider how the nucleation mode particles measured in the street canyon came to being? For example, if they are formed from the cooling of diesel exhaust as it leaves the tailpipe, could one envision a size dependent composition of the condensing species where the lower volatility species condense on smaller sizes from diffusion limited growth while the semi-volatile species condense on larger sizes from volume limited growth. Is it possible to measure the condensation of the hot/warm tailpipe emissions with this model before it is used to model the evaporation? What organic aerosol concentration was assumed to model gas/particle partitioning?

Answer: The same organic compound distribution is used for all particle sizes, however, the non-volatile fraction is different between the modes. Aitken mode particles are considered predominantly non-volatile (90% of their mass in non-volatile) and therefore their slow dynamics is of little interest. Nucleation mode particles (diameter less than 30 nm) and their composition, however, are still not fully understood. In this study we found that nucleation mode particles composed predominantly of highly volatile SVOC can explain the shrinkage behaviour seen in the observations of Dal'Osto et al (2011) in Central London. Our model is not capable of simulating exhaust hot tailpipe emissions, nor processes in the first stage of dilution with cleaner air. The

organic aerosol mass fraction is based on the Gaussian distribution (please refer to our Supplementary Information) and the total mass per size bin is estimated based on the observed number size distribution in Dal'Osto et al. (2011).Gas-phase concentration is based on the work of Harrad et al. (2003, see the reference list in the ms).

Minor comments:

1. Line 44, 62: No need for citations in the abstract

Answer: Because our study links closely to the two previous papers cited in the abstract, and the abstract must be able to stand alone, we respectfully request to retain sufficiently detailed citations, in line with best practice.

2. Line 89: Perhaps define SVOC using the effective saturation concentration definition (C) of Donahue et al. (2006) too?*

Answer: This section now reads (lines 89-92): 'Progress has been made in modelling traffic-generated particles (including the ultrafine fraction) using a volatility basis set, defined using the effective saturation concentration (Donahue et al., 2006). Progress in identifying the precise chemical composition of traffic-generated particles has been made by resolving the so-called 'unresolved complex mixture' (largely uncharacterised organics in traditional gas chromatography) via two-dimensional gas chromatography…'

Donahue et al., 2006, has been added to the references.

3. Line 107-110: Mention timescales over that 650m too?

Answer: We have added the following information on the travel time as follows (lines 118-119): 'The travel time, depending on the wind speed, can vary from about 100 s to 300 s.'

4. Line 117: How are the nucleation and Aiken modes defined?

Answer: We have added a description of the modes and the diameter size ranges in section Introduction, lines 75-77, as follows: 'Hereafter, nucleation mode particles are defined as particles with diameter less than 30 nm, Aitken mode particles have a diameter in the range 30 – 100 nm.'

5. Line 155-179: Is it possible that the organic species distribution is bimodal?

Answer: See answer to major comment 1, above. We cannot rule out multi-modal compositions where they are not well approximated by a single Gaussian. Our mono-modal organic compounds distribution is in line with the work of Alam et al. (2016) who observed mono-modal dustribution at the tailpipe (please refer to Figure 1 in our ms), and the additional references cited above.

6. Line 283: C20H42?

Answer: We do mean C20H42, but this is plotted with the green solid line *not* the purple. This is now corrected at line 307 as follows:' . For example, at $\sigma = 1$ and initial mass distribution centred at $C_{20}H_{42}$ (green solid line with a square marker), …'

7. Line 311: I am not sure I understand the comment about longer evaporation timescales for higher carbon number species. My understanding is that the higher carbon number species are already in equilibrium since they have a much lower C and they would only evaporate if the parcel was continuously diluting – which is not how the model in this work was setup. Can you clarify? Or are you referring to the fact that for two semi-volatile species, the larger species on account of its larger molecular weight/diffusion coefficient would evaporate slower?*

Answer: We refer to the fact that for two semi-volatile compounds, the largest in molecular weight compound would evaporate slower in comparison with the lightest in molecular weight compound. We have re-phrased the sentence in our manuscript at line 330ff: 'Furthermore, the timescales are much shorter for those lower than $C_{21}H_{44}$ carbon-number compositions (e.g. $C_{20}H_{42}$, $C_{19}H_{40}$, …)

and much longer for those higher than $C_{21}H_{44}$ carbon-number compositions (e.g. $C_{22}H_{46}$, $C_{23}H_{48}$,…).

8. I would have preferred to use non-volatile instead of involatile in the manuscript, based on the word choice see elsewhere in the literature. Is there a reason for using involatile?
Answer: There is no reason for using the word involatile. Literature studies use both words. For consistency with our previous work, all words 'involatile' are replaced with the word 'non-volatile' in our main and supplementary papers.

9. Line 336-343: What are the implications of this section?
Answer: This section aims to provide the reader with supportive information on the meaning of threshold modal composition based on our definition and approach.

10. Line 419: The authors mention the use of a size-resolved composition. However, I don't see this information visualized or tabulated anywhere in the manuscript. What am I missing?
Answer: All input information is presented in the Supplementary Information. The size-resolved composition can be found in Tables 1S-4S.

11. Line 483: As mentioned above, why wasn't the effect of dilution simulated in this work?
Answer: Mixing of cleaner urban background air into the simulated air parcel would lower partial pressures and increase evaporation rates. In our study the gas-phse SVOC data of Harrad et al (2003) is used to represent the urban air while the urban background gas-phase concentration is set to zero therefore observing a maximum decrease in particle diameter.

The influence of particle composition upon the evolution of urban ultrafine diesel particles on the neighbourhood scale

Irina Nikolova[1], Xiaoming Cai[1], Mohammed Salim Alam[1], Soheil Zeraati-Rezaei[2], Jian Zhong[1], A. Rob MacKenzie[1,3*] and Roy M. Harrison[1,4]

[1]School of Geography, Earth and Environmental Sciences
University of Birmingham, Edgbaston, Birmingham B15 2TT
United Kingdom

[2]Department of Mechanical Engineering
University of Birmingham, Edgbaston, Birmingham B15 2TT

United Kingdom

[3]Birmingham Institute of Forest Research (BIFoR)

University of Birmingham, Edgbaston, Birmingham B15 2TT

United Kingdom

[4]Also at: Department of Environmental Sciences / Center of Excellence in Environmental Studies, King Abdulaziz University, PO Box 80203, Jeddah, 21589, Saudi Arabia

[*] Corresponding author: a.r.mackenzie@bham.ac.uk

ABSTRACT

A recent study demonstrated that diesel particles in urban air undergo evaporative shrinkage

when advected to a cleaner atmosphere (Harrison et al., Atmospheric Environment, 2016, 125, 1-7). We explore, in a structured and systematic way, the sensitivity of nucleation-mode diesel particles (diameter $<$ 30 nm) to changes in particle composition and saturation vapour pressure. We use a multi-component aerosol microphysics model based on surrogate molecule (C_{16}-C_{32} n-alkane) volatilities. For standard atmospheric conditions (298 K, 1013.25hPa), and over timescales (ca. 100 s) relevant for dispersion on the neighbourhood scale (up to 1 km), the choice of a particular vapour pressure dataset changes the range of compounds that are appreciably volatile by 2-6 carbon numbers. The nucleation-mode peak diameter, after 100 s of model runtime, is sensitive to the vapour pressure parameterisations for particles with compositions centred on surrogate molecules between $C_{22}H_{46}$ and $C_{24}H_{50}$. The vapour pressure range is between 9.23×10^{-3} and 8.94×10^{-6} Pa for $C_{22}H_{46}$ and 2.26×10^{-3} and 2.46×10^{-7} Pa for $C_{24}H_{50}$. The vapour pressures of components in this range are therefore critical for the modelling of nucleation-mode aerosol dynamics on the neighbourhood scale and need to be better constrained. Laboratory studies have shown this carbon number fraction to derive predominantly from engine lubricating oil. The accuracy of vapour pressure data for other (more and less volatile) components from laboratory experiments, is less critical. The influence of a core of non-volatile material is also considered.

The new findings of this study may also be used to identify the Semi-Volatile Organic Compound (SVOC) compositions that play dominating roles in the evaporative shrinkage of the nucleation mode observed in field measurements (Dall'Osto, et al., Atmospheric Chemistry & Physics, 2011, 11, 6623-6637).

1. INTRODUCTION

Ultrafine particles (UFP, with particle diameter Dp < 100 nm) have been increasingly a focus of urban air research over the last two decades. The main source of UFP in outdoor urban air is typically road traffic (Kumar et al., 2014). Harrison et al. (2011) reported that on a busy highway in central London, UK, 71.9% of particles by number were traffic-generated; of which 27.4% are found in the semi-volatile exhaust nucleation mode (size between 15 and 30 nm), 38% are in the exhaust solid mode (size > 30 nm) and the remaining 6.5% are from brake dust and resuspension (size > 2000 nm). Hereafter, nucleation mode particles are defined as particles with diameter less than 30 nm, Aitken mode particles have a diameter in the range 30 – 100 nm. The proximity of the UFP traffic source to the public, and the large number of UFP emitted by traffic, have prompted health-related research that has accrued evidence pointing to the toxicity and potentially harmful effects of UFP on human health (Atkinson et al., 2010). Experimental and modelling studies have advanced our understanding of the behaviour of urban air UFP, e.g. the relevant aerosol dynamics important to the evolution of the UFP in space and time (Jacobson, 2005; Allen et al., 2007; Biswas et al., 2007; Dall'Osto et al., 2011; Nikolova et al., 2011; Karnezi et al, 2014, Karl et al., 2016).

Nonetheless, key information regarding the size-resolved composition of the UFP is missing, which limits our ability to determine the impact of gas-transfer processes on UFP evolution. Progress has been made in modelling traffic-generated particles (including the ultrafine fraction) using a volatility basis set, defined using the effective saturation concentration (Donahue et al., 2006). Progress in identifying the precise chemical composition of traffic-generated particles has been made by resolving the so-called ‘unresolved complex mixture’ (largely uncharacterised organics in traditional gas chromatography) via two-dimensional gas chromatography (GC×GC; Chan et al., 2013). Alam et al. (2016) show that emitted ultrafine diesel particles consist of a substantial amount of organic material from both unburnt diesel fuel and engine lubricating oil. They attribute the low molecular weight Semi-Volatile Organic Compounds (SVOCs, having carbon number < 18) predominantly to the unburnt diesel fuel, whereas heavier SVOCs (carbon

number > 18) are attributed predominantly to the engine lubricating oil. A typical GC×GC separation is shown in the chromatogram (Figure 1) for diesel engine exhaust emissions in the particulate-phase Aitken mode (56 < D p< 100 nm). Compounds are separated by volatility along the *x*-axis (first separation dimension) and by polarity in the *y*-axis (second dimension). Peak identification is based on retention indices and mass spectral data from the National Institute of Standards and Technology (NIST) library. The majority of chromatography peaks (identified as aliphatic alkanes, lower black polygons) are present between C_{18} to C_{26}, corresponding to the compounds identified in the engine lubricating oil and particulate phase engine emissions (Alam et al. 2017). Bar charts above the chromatogram show the volatility distribution of total alkanes (red) and total identified compounds (black), indicating that, although many hundreds of individual chemical compounds are detected, the majority of the SVOCs emissions consist of alkanes. Both the alkane composition and the total composition distributions show a broad peak centred at C_{25}.

Most primary organic particle emissions are semi-volatile in nature and thus they are likely to evaporate with atmospheric dilution and moving away from the source (Robinson et al., 2007). This has been observed by Dall'Osto et al. (2011; see also Figure 1- S in Supplementary Information) as part of the REPARTEE campaign (Harrison et al., 2012). Dall'Osto et al. (2011) reported a remarkable decrease in the measured nucleation-mode peak particle diameter ($D_{pg,nuc}$) between a street canyon ($D_{pg,nuc}$ = 23 nm) and the downwind neighbourhood ($D_{pg,nuc}$ = 8-9 nm) ca. 650 m distant in central London (UK). The travel time, depending on the wind speed, can vary from ~100 s to ~ 300 s. Nucleation formation of new particles in the atmosphere was ruled out as a possible reason for the observed behaviour. Instead, the decrease in particle diameter was attributed to the effect of evaporation and substantial mass loss from the particle surface (hereafter referred to as REPARTEE-like aerosol dynamics). Alam et al. (2016) present the composition of diesel UFP particles measured on a laboratory test-rig (cf. Figure 2-S in Supplementary Information), however the range of variability of the particle composition in emissions is still unknown. It is also not known how the organic material is distributed onto the

nucleation and Aitken modes of the UFP distribution in the atmosphere.

Numerical experiments can test the plausibility of possible missing components of the system, and can advise on which experimental studies will be most likely to resolve the existing knowledge gaps. Nikolova et al. (2016) describe a modelling framework that can produce nucleation-mode dynamics consistent with observations. However, missing in that study is the identification of critical thermodynamic parameters and size-resolved composition that could determine or point to a REPARTEE-like aerosol dynamics.

In the present study, we develop a method to search the particle composition space — i.e. the volatility parameter space — to identify a group of surrogate n-alkanes in the $C_{16}H_{34}$-$C_{32}H_{66}$ range that could explain a decrease in the nucleation-mode particle diameter to 10 nm or below as seen in the measurements in London (Dall'Osto et al., 2011). The model simulations are focused on events after dilution and cooling of the exhaust-pipe plume. We provide a more robust approach to identify crucial parameters responsible for the UFP behaviour in the atmosphere on the neighbourhood scale including the identification of parameter sets that are incompatible with the observed behaviour in urban air of nucleation mode UFP. We describe a new way to simulate and evaluate the role of the SVOCs composition on the atmospheric behaviour of the size-resolved urban UFP and examine more complex sets of composition involving a non-volatile core. We also assess the critical role of saturation vapour pressure on the size-resolved aerosol dynamics.

In this study we use Lagrangian box-model simulations of the evolution of urban ultrafine diesel particles on the neighbourhood scale (up to 1 km). Key results will be presented and discussed in the main text; more details are provided in the Supplementary Information. The Methodology section describes the modelling approach. The Results section presents the model output. In the Discussion and Conclusions sections, the key findings are summarised with suggestions for further work.

2. METHODOLOGY

We adopt a 'surrogate molecule' approach to UFP composition, based on the chemical speciation shown in analyses such as Figure 1. The composition of UFP is simulated as comprising n-alkanes from $C_{16}H_{34}$ to $C_{32}H_{66}$, which are the most abundant compounds in Figure 1. Previously (Nikolova et al., 2016), we initialised the n-alkane abundance in gas and particle phases using roadside and urban background observations in Birmingham, U.K. (Harrad et al., 2003). In what follows, we retain this roadside gas-phase initialisation (see below), but choose a more general method for initialising the particle composition, in order to test the sensitivity of the results to the initialisation in a systematic way. By adopting a surrogate molecule approach, we are effectively anchoring the model volatility basis set in physico-chemical data, as discussed further below.

The SVOC mass fractions in a particle are represented by a truncated Gaussian distribution that is centred for each model run at a given n-alkane in the range from $C_{16}H_{34}$ to $C_{32}H_{66}$ with a standard deviation, σ, varying from 1 to 5. Below we call the surrogate n-alkane on which the composition distribution is centred, the *modal composition*. Example compositions are shown in Figure 2 for a Gaussian distribution centred at $C_{24}H_{50}$. A narrower mass distribution, with $\sigma = 1$, focuses predominantly (ca. 40%) on the component, j ($C_{24}H_{50}$), at which the distribution is centred, with a smaller (ca. 24%) contribution from the adjacent compounds $C_{23}H_{48}$ and $C_{25}H_{52}$, and a minor contribution (ca. 5%) from $C_{22}H_{46}$ and $C_{26}H_{54}$. The contribution of the remaining compounds from the tail of the distribution is very low and less than 1%. However, a wider mass distribution (e.g. $\sigma = 5$) approximates a flat distribution and includes a contribution from the majority or all of the compounds in the n-alkane range $C_{16}H_{34}$-$C_{32}H_{66}$. Monotonically decreasing distributions occur for distributions centred at either end of the $C_{16}H_{34}$-$C_{32}H_{66}$ range. Overall, if one excludes the compounds with less than 1% contribution, modal compositions centred at carbon number, j, with $\sigma = 1, 2, 3, 4, \& 5$, contain surrogate compounds +/- 2, 4, 7, 9, and 11 carbon numbers of j (formally, to remain in the 16-32 carbon number range, [max(16, j-2):min(32, j+2)], [max(16, j-4):min(32, j+4)], [max(16, j-7):min(32, j+7], [max(16, j-9):min(32, j+9], & [max(16, j-

11):min(32, j+11)]), respectively. Multi-modal compositions, or others differing strongly from Gaussian, are not investigated in the present study, but could be accommodated by a simple extension of the method.

We use a Gaussian distribution to represent the composition of the particles because it provides a structured and systematic way to evaluate the organic-aerosol phase partitioning and the amount of organic matter in the UFP. This is important for the behaviour and evolution of the UFP at various timescales relevant for the urban atmosphere. Although there is no reason to discount other functional forms for the composition distribution (e.g., skew Gaussian, log-normal, Pareto, linear, etc), the Gaussian distributions chosen represent a simple two-parameter approach to explore the volatility/composition space available.

2.1 Box Model

The model used in this study is the UFP version (Nikolova et al., 2016) of CiTTy-Street (Pugh et al., 2012); that is, a box-model configuration that accounts for the multicomponent nature of the urban ultrafine particles. The CiTTy-Street-UFP model is used with 15 discrete size bins, with an initial diameter range between 5.8-578 nm in a uniform log-scale. The model can operate in two modes with respect to the aerosol dynamics: Eulerian (fixed particle-diameter grid) or Lagrangian (moving particle-diameter grid). The Eulerian mode is selected when the UFP size distribution is evaluated in the presence of emissions and exchange of particles between boxes (Nikolova et al., 2016). The Lagrangian mode can be selected when the UFP size distribution is evaluated for an isolated air parcel, i.e., when no emissions or transport between boxes are present. In this study, the Lagrangian mode is selected in a zero-dimensional configuration with no emissions or transport in/out of the box. The UFP dynamics (only condensation/evaporation) are simulated such that particles are allowed to grow/shrink to their exact size without any redistribution onto fixed bins in a grid with bin bounds left open in a fully moving diameter scheme (see, for example, Jacobson et al., 1997). Our earlier work (Nikolova et al., 2016) has shown that deposition and coagulation have a minor effect in the current scenario and so were switched off to

allow a more straightforward diagnosis of model behaviour. The condensation/evaporation process applies Raoult's Law (for an ideal solution of the volatile compounds) and a mass accommodation coefficient $\alpha = 1$ (Julin et al., 2014) for all SVOC. The Kelvin effect is also considered, which alters the saturation vapour pressure of the compounds as a function of the particle diameter, the surface tension of the SVOC mixture/solution, and the molecular weight of the participating compounds. The Kelvin effect is pronounced for particles with a diameter less than 20 nm and substantial for particles with diameter less than 10 nm. The Kelvin term accelerates the evaporation for all compounds under consideration in this study and more notably for the high-molecular-weight compounds due to their larger molar volume.

The model results are evaluated at 1, 10 and 100 s. The timescale of 100 s is based on estimate of the travel time on the neighbourhood scale (i.e., horizontal travel distances << 1 km).

2.2 Modal Composition and Initial Size-Resolved UFP distribution

The initial size-resolved UFP distribution is based on the measurements of Dall'Osto et al. (2011) and reproduced in Figure 1-S in the Supplementary Information. This ultrafine size distribution represents the typical street canyon bimodal size distribution found next to a traffic site, e.g. next to Marylebone Road in London (UK). The distribution has a well-defined nucleation mode with a peak number concentration at $D_{pg,nuc} \sim 23$-24 nm. The Aitken mode appears as a shoulder attached to the nucleation mode with a peak number concentration found at $D_{pg,aim}$ between 50-60 nm.

The initial UFP size-resolved composition is represented by modal compositions in the range $C_{16}H_{34}$-$C_{32}H_{66}$, as detailed above, and a standard deviation σ from 1 to 5. A non-volatile core is included in the ultrafine particles. While studies broadly agree on the existence of a non-volatile core in the Aitken mode (Biswas et al., 2007; Wehner et al., 2004; Ronkko et al., 2013), it is unclear if nucleation-mode particles contain some non-volatile material or if they are entirely composed of (semi-)volatile SVOC. We have tested the sensitivity to the existence of non-volatile material in the nucleation mode particles by initialising with 1%, 5% or 10% by mass non-volatile material for each modal composition (see Supplementary Information for details of the initialisation); results are discussed later in this paper. Simulations are performed by

considering the initialised Aitken mode predominantly non-volatile and coated only with 10% volatile material. This is based on the observations during the REPARTEE campaign (Harrison et al., 2012) that show a fairly stable Aitken mode between the street canyon and the neighbourhood. The initial size-resolved modal compositions, composition standard deviations and non-volatile core in the nucleation and Aitken modes are detailed in Tables 1-S, 2-S, 3-S and 4-S in the Supplementary Information. We also provide information on the input parameters of the log-normal UFP size distribution for Nucleation and Aitken modes.

2.3 Saturation Vapour Pressures and Gas-Phase Concentrations

The driving force for condensation/evaporation is the difference between the partial pressure of each representative SVOC and its saturation vapour pressure (hereafter vapour pressure) over the ideal solution in the nucleation mode condensed phase. Figure 3 shows vapour pressures above pure, flat, supercooled liquids for n-alkanes in the range $C_{16}H_{34}$-$C_{32}H_{66}$, following Chickos and Lipkind (2008), Compernolle et al. (2011), Lemmon and Goodwin (2000), the Epi Suite calculator (US EPA, 2017), and the UmanSysProp tool (Topping et al., 2016). The UmanSysProp tool provides vapour pressure data based on the work of Nannoolal et al. (2008) and Myrdal and Yalkowsky (1997) with the boiling points of Joback and Reid (1987), Stein and Brown (1994), and Nannoolal et al. (2004). There is a very substantial range of estimated vapour pressures for the same compounds in Figure 3, especially for the high molecular weight n-alkanes. The reported data agrees within an order of magnitude between $C_{16}H_{34}$ and $C_{19}H_{40}$, but discrepancies of much more than an order of magnitude are evident for the high molecular weight compounds. The vapour pressure ranges of $C_{22}H_{46}$ and $C_{24}H_{50}$ are between [9.23×10^{-3} and 8.94×10^{-6} Pa] and [2.26×10^{-3} and 2.46×10^{-7} Pa], respectively. An enormous difference in the vapour pressure for $C_{32}H_{66}$ (from 2.66×10^{-5} Pa in Epi Suite, to 3.20×10^{-15} Pa in Nannoolal et al., 2008 with the boiling point of Joback and Reid, 1987, called A-a hereafter) is clearly seen in Figure 3. Epi Suite (U.S. Environmental Protection Agency) provides the highest vapour pressures for all selected species in comparison with the rest of the data. Nannoolal et al. (2008) and Myrdal-Yalkowsky (1997) data, both using the boiling point of Joback and Reid (1987), provide similar results and present

the lowest vapour pressures among the selected n-alkanes. For the purpose of our sensitivity study, three representative datasets are nominated as input, namely: Myrdal-Yalkowsky (1997) with the boiling point of Nannoolal et al. (2004, called B-c in Figure 3 and hereafter); Compernolle et al. (2011, called Co); and A-a. Hereafter we use the legend abbreviations in Figure 3 when referring to these selected vapour pressures, which are towards the upper, mid- and lower end of the reported data. The vapour pressure from the EPI Suite calculator has been omitted from the analysis below because it has been considered in our previous study (Nikolova et al., 2016).

The gas-phase concentration in the box is initialised with measured gas-phase concentrations in the $C_{16}H_{34}$-$C_{32}H_{66}$ range from a traffic site (Harrad et al., 2003) and reported in Table 6-S in the Supplementary Information. For hydroxyl (OH) radical concentration ~10^6 molec cm^{-3}, the timescale for atmospheric oxidation of $C_{16}H_{34}$ is about 10^6 s (Atkinson and Arey, 2003). Therefore oxidation of SVOC is neglected given the timescale in our study (100 s). The urban background gas-phase concentration is kept at zero. All model simulations are run at 298 K; the effects of temperature on vapour pressure differences as a function of carbon number are discussed in the Supplementary Information.

We have performed a total of (17 modal compositions) x (5 σ values) x (3 non-volatile core amounts) x (3 vapour pressures) = 765 model runs to explore the sensitivity of particle dynamics on the neighbourhood scale.

The Supplementary Information contains information regarding the initial size distribution, modal composition in the nucleation and Aitken modes, and gas-phase concentrations. Accumulation-mode aerosol (particles diameter Dp > 100 nm) is not considered in this study. Accumulation-mode particles have much smaller number concentrations than the nucleation and Aitken modes in polluted urban areas, and are influenced by aging and transport over larger scales.

3. RESULTS

3.1 Effect of composition on Nucleation-Mode Peak Diameter

We consider first model runs in which the vapour pressure data follows Co (Compernolle et al. (2011) and nucleation mode particles initialised with 1% non-volatile material. The nucleation mode peak diameter $D_{pg,nuc}$ is evaluated at 1 s and 100 s of model run-time in runs with varying modal composition and composition standard deviations. Figure 4 shows $D_{pg,nuc}$ (y-axis) at 1s simulation time, for each model run, plotted with respect to the modal composition and composition standard deviation, σ.

Figure 4 maps out the effect of nucleation-mode composition at this very early stage in the model simulation. For example, at σ = 1 and initial mass distribution centred at $C_{20}H_{42}$ (green solid line with a square marker), the $D_{pg,nuc}$ decreased from 23 nm (initial diameter at t = 0 s) to 12 nm in one second due to evaporation of volatile material from the particles. At σ = 2, $D_{pg,nuc}$ = 15 nm, a somewhat larger diameter than for σ = 1, due to the inclusion of material of lesser volatility in the particle composition and, hence, a decrease in evaporation overall. For modal compositions between $C_{16}H_{34}$ and $C_{20}H_{44}$, an increase in σ leads to a pronounced deceleration in overall evaporation and, hence, a much larger nucleation mode peak diameter at 1 s simulation time. The opposite effect occurs for modal compositions of $C_{22}H_{46}$ and above, i.e. increasing σ for a given modal composition decreases $D_{pg,nuc}$ at 1 s. This is due to the addition of quickly evaporating lower molecular weight n-alkanes.

For a modal composition of $C_{21}H_{44}$, increasing σ makes almost no difference to the model outcome at 1 s. Below, we call the modal composition that shows insensitivity to σ for a given model output time, the *threshold modal composition*. The threshold modal composition points to the composition compound that is in equilibrium between gas and particulate phases for the selected timescale. Lower-carbon-number compositions than the threshold modal composition evaporate quicker and therefore have reached equilibrium with their respective gas concentrations

on a much shorter timescale. The higher-carbon-number compositions evaporate slowly and are out-of-equilibrium with their respective gas concentrations for the selected timescale.

The model output time of 1 s corresponds to the evaporation timescale of $C_{21}H_{44}$ under the current model setting, in analogy to the e-folding time for an exponentially decaying process. That is, at this time, a significant proportion (e.g. $1\text{-}e^{-1} \sim 63\%$ for one e-folding time, and $1\text{-}e^{-2} \sim 86\%$ for two e-folding times) of the initial mass has been evaporated. Furthermore, the timescales are much shorter for those lower than $C_{21}H_{44}$ carbon-number compositions (e.g. $C_{20}H_{42}$, $C_{19}H_{40}$, …) and much longer for those higher than $C_{21}H_{44}$ carbon-number compositions (e.g. $C_{22}H_{46}$, $C_{23}H_{48}$,…).

To continue the previous example of the modal composition of $C_{20}H_{42}$, the case with $\sigma = 2$ includes not only less volatile materials (i.e. higher-carbon-number SVOCs), but also an equal amount of more volatile materials (i.e. lower-carbon-number SVOCs), as indicated by Figure 2. One might suppose that inclusion of the more volatile material would balance the effect of including less volatile materials. However, following our argument above, most of the lower-carbon-number compounds including $C_{20}H_{42}$ will have evaporated before the given time of 1 s due to their having much shorter evaporation timescales than $C_{21}H_{44}$. Thus any material repartitioned from $C_{20}H_{42}$ to the lower-carbon-number compounds, in changing the model settings from to $\sigma = 1$ to $\sigma = 2$, will not alter the total amount of evaporation and thus the shrinkage rate.

To take a second example: for $C_{22}H_{46}$, any material reallocated from $C_{22}H_{46}$ to the higher-carbon-number compounds (due to changing the model setting from $\sigma = 1$ to $\sigma = 2$) will contribute negligibly to the shrinkage simply because the evaporation timescales for those higher-carbon-number components are much longer than 1 s, whilst the materials repartitioned from $C_{22}H_{46}$ to the lower-carbon compounds will contribute significantly to evaporation in the first second of model run-time, causing the decreasing trend of the curve shown in Figure 4.

One implication of this finding is that, if a timescale of 1 s is of interest, the aerosol dynamics of the system is dominated by the threshold modal composition of $C_{21}H_{44}$. Those lower-carbon-number compositions evaporate in less than 1 s and are approximately in equilibrium with their respective gas concentrations in the environment. The higher-carbon-number compositions evaporate slowly and at this time of 1 s, only a small or a negligible proportion has been evaporated. A few compositions with highest carbon numbers (e.g. $C_{31}H_{64}$, $C_{32}H_{66}$) have evaporated almost nothing. Therefore these compositions are effectively non-volatile for these conditions.

Nucleation-mode particles have an initial non-volatile mass of 2.9 ng m^{-3}. Modal compositions from $C_{16}H_{34}$ to $C_{19}H_{40}$ and $\sigma = 1$ will lose all their volatile mass in 1 s (Table 1). The initial $D_{pg,nuc}$ decreases from 23 nm to 9 nm and no volatile material is present, i.e. particles are composed of non-volatile core only. Little or no change is simulated in terms of mass and diameter for modal composition $C_{32}H_{66}$.

At 100 s, the evaporation of existing mass from the surface of the particles is evident also for higher molecular weight components (Table 1). The $D_{pg,nuc}$ at 100 s is plotted in Figure 5. The diameter has further decreased with a more pronounced drop for all σ and modal compositions up to $C_{25}H_{52}$. $C_{25}H_{52}$ is, therefore, the threshold modal composition at this model output time.

The horizontal line drawn at 10nm on Figure 5 corresponds to evaporation approximating REPARTEE-like behaviour. At $\sigma = 1$, modal compositions in the range $C_{16}H_{34}$-$C_{23}H_{48}$ — and vapour pressures and gas-phase partial pressures as detailed in the methodology — could plausibly explain a particle diameter decrease from 23 nm to ~9 nm. Such a narrow range of surrogate molecular compounds is incompatible with experimental observations such as Figure 1. At $\sigma = 2$ and $\sigma = 3$, modal compositions from $C_{16}H_{34}$ up to $C_{22}H_{46}$ and $C_{21}H_{44}$, respectively, can plausibly approximate REPARTEE-like behaviour. At $\sigma = 4$ and $\sigma = 5$ modal compositions from

$C_{16}H_{34}$ up to $C_{19}H_{40}$ and $C_{17}H_{36}$, respectively, plausibly simulate REPARTEE-like behaviour.

3.2 Effect of Vapour Pressure on the Nucleation-Mode Peak Diameter

We compare the simulated nucleation-mode peak diameter, $D_{pg,nuc}$, at 100 s using the vapour pressure parameterisations B-c, Co and A-a (cf. Figure 3). The nucleation mode particles are initialised with 1% non-volatile material in these simulations. Diameter change when using Co vapour pressure has been discussed in the previous section. The values of vapour pressure in the Co data are intermediate between the B-c and A-a data. Hence, $D_{pg,nuc}$ at 100 s using vapour pressure parameterisations A-a and B-c (see Supplementary Information), as expected, shows the same general behaviour as for vapour pressure parameterisation Co, but with a marked change in threshold modal composition. In order of decreasing vapour pressure (Figure 3), the threshold modal composition value changes from $C_{27}H_{56}$ for the B-c parameterisation (Figure 4-S in the Supplementary Information), to $C_{25}H_{52}$ for Co (Figure 5), to $C_{22}H_{46}$ for A-a (Figure 5-S in the Supplementary Information). We restrict ourselves to integer values of threshold modal composition to maintain a straightforward connection back to the homologous chemical series in Figure 1, although there is nothing in principle to prevent us from attributing real number values to the threshold modal composition.

There is no composition with $\sigma = 4$ and $\sigma = 5$, at the lower volatility A-a vapour pressure parameterisation, that produces REPARTEE-like behaviour; i.e., decrease of the nucleation-mode peak diameter from 23 nm to 10 nm or below. At $\sigma = 5$, the nucleation-mode particles can lose a maximum of ~9 nm of their initial diameter for modal composition $C_{16}H_{34}$ (please refer to Figure 5-S in the Supplementary Information). Little or no change in mode diameter is simulated for modal compositions between $C_{24}H_{50}$ and $C_{32}H_{66}$ and $\sigma = 1$, indicating that these combinations of composition and vapour pressure parameterisation are essentially non-volatile for the 100 s simulation time. Modal compositions $C_{20}H_{42}$ ($\sigma = 1$), $C_{19}H_{40}$ ($\sigma = 2$) and $C_{17}H_{36}$ ($\sigma = 3$) can produce REPARTEE-like aerosol dynamics.

Vapour pressure parameterisation B-c has the highest vapour pressure for all compounds in comparison with Co and A-a. Hence, particles in the nucleation mode are subject to a more pronounced evaporation, even for modal compositions $C_{28}H_{58}$ to $C_{32}H_{66}$. Nonetheless, only modal compositions $C_{25}H_{52}$ ($\sigma = 1$), $C_{24}H_{50}$ ($\sigma = 2$), $C_{23}H_{48}$ ($\sigma = 3$), $C_{21}H_{44}$ ($\sigma = 4$) and $C_{20}H_{42}$ ($\sigma = 5$) are able to produce the REPARTEE-like behaviour. Table 2 provides details on the modal compositions and composition standard deviations that approximate the REPARTEE-like aerosol dynamics for B-c, Co and A-a vapour pressure parameterisations.

The difference in 100-s $D_{pg,nuc}$ between the highest vapour pressure (B-c) and the lowest vapour pressure (A-a) for all values of σ, is shown in Figure 6. The largest differences (10-14 nm) between the $D_{pg,nuc}$ occur for modal compositions between $C_{22}H_{46}$ and $C_{24}H_{50}$ and $\sigma = 1, 2, 3$. For model run-time of 100 s, the variability of the UFP shrinkage due to the uncertainty of vapour pressure data is highest for the compositions between $C_{22}H_{46}$ and $C_{24}H_{50}$. From Figure 3, we see that the uncertainty of vapour pressure data increases monotonically with carbon number and is highest for $C_{32}H_{66}$. However this high level of uncertainty for high-carbon compositions does not exert a significant impact on the model results. We thus conclude that the accuracy of vapour pressure values for very high or very low carbon compositions are not important for neighbourhood-scale aerosol dynamics.

3.3 Effect of Non-Volatile Core on the Nucleation Mode Peak Particle Diameter

To consider how the fraction of non-volatile core interacts with the SVOCs composition and the vapour pressure parameterisations, we define a '100-s effective non-volatile core': the nucleation mode peak diameter at 100 s of evaporation. Figure 7 shows results for three non-volatile fractions (initial1%, 5% and 10% based on mass) and vapour pressures A-a, B-c and Co (cf. Figure 3), for a modal composition of $C_{16}H_{34}$. Results for the remaining modal compositions are not plotted here because using modal composition $C_{16}H_{34}$ and an evaporation time of 100 s gives the maximum reduction of the nucleation-mode peak diameter for all σ in our model runs. However, we show the results for modal compositions $C_{24}H_{50}$ and $C_{32}H_{66}$ for completeness in the

Supplementary Information (Figure 7-S).

Because the mass-size distribution is held constant for each model initialisation (see Supplementary Information), an increase of the non-volatile material in the nucleation mode leads to a decrease in the total amount of n-alkane SVOC available for evaporation, and hence leads to an increase in the nucleation mode 'dry' (i.e. non-volatile core only) diameter from ~9 nm to ~12 nm. For the lowest volatility parameterisation (A-a), only the lightest surrogate compounds near $C_{16}H_{34}$ are sufficiently volatile over the timescale of the model run to drive evaporation of nucleation mode particles. As σ increases, an increasing number of lower volatility components are added into the particle composition, causing the 100-s effective non-volatile core to increase.

Considering REPARTEE-like behaviour, i.e., shrinkage of the nucleation mode diameter to ca. 10 nm, initial non-volatile core fractions of 5% or greater do not reproduce the observed behaviour.

4. DISCUSSION AND CONCLUSIONS

The purpose of this study was to evaluate the importance of particle composition and saturation vapour pressure on the evolution of urban ultrafine diesel particles on the neighbourhood scale (<< 1 km) by means of numerical simulations. We present the effect of evaporation on the size-resolved ultrafine particles and looked at the evolution of the nucleation-mode peak diameter $D_{pg,nuc}$ depending on particle SVOC composition, vapour pressure, and fraction of non-volatile core in the particles. We have used laboratory measurements of the size-resolved composition of the ultrafine particles as an additional strong constraint on the plausibility of model parameter sets. We identified a group of surrogate n-alkane compounds in the range $C_{16}H_{34}$-$C_{32}H_{66}$ that could explain REPARTEE-like aerosol dynamics measured in London (Dall'Osto et al., 2011): i.e., a final nucleation-mode peak diameter at 10 nm or below when particles were subject to

evaporation in a timescale of 100 s. Table 2 highlighted the set of parameters in terms of vapour pressure and modal compositions that produce such REPARTEE-like behaviour.

Table 2 presents the sets of model parameters consistent with diameter reduction due to evaporation. The question remains, however, to what extent these results are realistic and relevant for the real-world atmosphere. Standard deviation $\sigma = 1$ for all vapour pressures narrows significantly the contribution from the n-alkanes ([max(16, j-2):min(32, j+2)] for modal composition j), present in the initial composition of the nucleation mode particles. At $\sigma = 2$, the main contributing compounds involved in particle composition are the modal composition j and the surrogate molecules [max(16, j-4):min(32, j+4)]. This means that for the given vapour pressure parameterisation, A-a, and modal composition $C_{19}H_{40}$, the compounds found in the particles would be between $C_{15}H_{32}$ and $C_{23}H_{48}$.\ However, $C_{16}H_{34}$ is the lower limit of surrogate compounds in the model, so the Gaussian distribution of composition is truncated at the low-carbon-number end in this case. At $\sigma = 3$, the contributing compounds found in the particles are the surrogate molecules in the range [max(16, j-7):min(32, j+7)]. For a modal composition $C_{17}H_{36}$ and A-a vapour pressure, the range of participating compounds is $C_{16}H_{34}$-$C_{24}H_{50}$, similar to the case of $\sigma = 2$. At $\sigma = 4$ and 5, the majority of the surrogate molecules in our range of n-alkanes participate in the composition of particles, thus providing a reasonable range over the contribution from diesel fuel and engine lubricating oil. The range at $\sigma = 3$ could be considered as a transition range, while examples at $\sigma = 2$ would have compositions that are rather more limited than available measurements in the Aitken mode (e.g. Figure 1), with a focus on the contribution from the engine lubricating oil. Overall, narrow compositions would imply a strong gradient of SVOCs across the nucleation and Aitken modes whereas broad compositions imply that SVOCs are more or less evenly distributed across the ultrafine size range.

Table 3 shows an additionally constrained range of modal compositions consistent with what we know from field and laboratory measurements combined. The lowest vapour pressure parameterisations (A-a and the very similar B-a, see Figure 3) are less likely, at any modal composition standard deviation (σ), to represent the laboratory and field observations together.

The results reported in Alam et al. (2016) and in Figure 1 show that diesel ultrafine particle emissions are composed of a wealth of SVOCs that are mainly identified as straight and branched alkanes in the range C_{11}-C_{33}, cycloalkanes (C_{11}-C_{25}), PAHs, various cyclic aromatics, alkyl benzenes and decalins. They report emitted particulate size fractionated concentrations of n-alkanes (cf. Figure 2-S in Supplementary Information) and point out that particles in the 5-100nm diameter range consist mainly of high molecular weight SVOCs (>$C_{24}H_{50}$) associated with engine lubricating oil. The work of Robinson et al. (2007), Grishop et al. (2009) and May et al. (2013) also point to a Gaussian-type distribution of the exhaust particle composition centred at SVOC, that has a wide standard deviation.

Vapour pressure parameterisations used in this study and plotted in Figure 3, are one of the crucial input parameters in assessing the rate at which condensation/evaporation can occur, though they are poorly constrained. We introduced a new concept of threshold modal composition, i.e. modal composition that is not sensitive to σ for a given model output time. In an order of decreasing vapour pressure (Figure 3) and timescale of 100 s, the threshold modal composition value changes from $C_{27}H_{56}$ for the B-c parameterisation (Figure 4-S, Supplementary Information), to $C_{25}H_{52}$ for Co (Figure 5), to $C_{22}H_{46}$ for A-a (Figure 5-S, Supplementary Information). Overall, the largest differences (~14 nm) in the 100-s $D_{pg,nuc}$ occur between the highest (B-c) and the lowest (A-a) vapour pressure parameterisations for modal compositions between $C_{22}H_{46}$ and $C_{24}H_{50}$ and composition standard deviation from 1 to 3. The vapour pressures of components in this range are therefore critical for the modelling of nucleation-mode aerosol dynamics on the neighbourhood scale. For components with volatility less than that for the $C_{22}H_{46}$ surrogate compound used here, all available vapour pressure parameterisations render these compounds volatile over the 100-s timescale. These components will equilibrate with the gas phase on these short timescales. Components with volatility lower than that of the $C_{24}H_{50}$ surrogate are effectively non-volatile over this timescale for all vapour pressure parameterisations, and so will remain condensed and out-of-equilibrium with the gas phase on

these timescales.

The other variable which will influence evaporation rate is the concentration of vapour surrounding the particles. In this work, measured roadside vapour concentrations reported by Harrad et al. (2003) are used (see also Nikolova et al., 2016). These represent an upper estimate of gas-phase partial pressures away from roadside. Mixing of cleaner urban background air into the simulated air parcel would lower partial pressures and increase evaporation rates.

The 100-s effective non-volatile core (the nucleation mode peak diameter at 100 s of evaporation) increased from ~9 nm to ~12 nm. This was attributed to the decrease in the total amount of n-alkane surrogate compounds present for evaporation. As composition standard deviation σ increased, an increasing number of lower volatility components added into the particle composition caused the 100-s effective non-volatile core to further increase. Considering REPARTEE-like behaviour, i.e., shrinkage of the nucleation mode diameter to ca. 10 nm, an initial non-volatile core of 5% by mass or greater was not capable of reproducing the observed behaviour in the atmosphere. Because the higher molecular weight (lower volatility) surrogate molecules in the model are essentially non-volatile over the modelling timescale, the nucleation mode dynamics due to SVOC is confounded with that due to the size of any non-volatile core present in the particles.

Results (Figure 7) suggest that urban nucleation mode particles should be predominantly volatile in order to produce REPARTEE-like behaviour. In these numerical experiments, the nature of the non-volatile core need not be specified. This core could be composed of one or more low vapour pressure compounds, not affected by condensation/evaporation on the timescale of the model and measurements. On the other hand, as discussed in Nikolova et al. (2016), a non-volatile core could be composed mainly of carbon and possibly some contribution from metal oxides and sulphates. This difference in composition could be relevant to effects on human health. Li et al. (2010) show that diesel truck emissions during idle induce a high level of oxidative stress in

human aortic endothelial cells, due to the type of metals and trace metals found in the exhaust, while Xia et al. (2015) argue that traffic-related UFP act to promote airway inflammation due to the rich content of organic species. The relative importance of these particles in affecting human health merits further investigations.

Laboratory exhaust diesel ultrafine particulate measurements are highly dependent on the sampling methods. Measurements of the ultrafine particle composition from a diesel-fuelled engine are still at an early stage and therefore more efforts should be put into developing sampling protocols that target the composition of the nucleation and Aitken modes particles in a realistic manner. There are no robust UFP chemical composition measurements at street scale and therefore such measurements devoted to address in detail the composition of the traffic emitted UFP in the atmosphere are urgently needed. Saturation vapour pressure is another source of large uncertainties; our study lays out a strategy to determine which vapour pressures are most significant in a given modelling scenario.

ACKNOWLEDGEMENTS

This work is part of the FASTER project, ERC-2012-AdG, Proposal No. 320821 sponsored by the European Research Council (ERC).

REFERENCES

Alam, M. S, Rezaei, S. Z., Stark, C. P., Liang, Z., Xu, H. M. and Harrison, R. M.: The characterisation of diesel exhaust particles – composition, size distribution and partitioning, Faraday Discuss., 189, 69-84, 2016.

Alam, M. S., Liang, Z., Rezaei, S. Z., Stark, C. P., Xu, H. M., MacKenzie, A. R. and Harrison, R. M.: Mapping and quantifying isomer sets of hydrocarbons (≥C12) in diesel fuel, lubricating oil and diesel exhaust samples using GC×GC-ToFMS, Atmos. Meas. Tech. Discuss., submitted, 2017.

Allen, L. R., Donahue, N. M., Shrivastava, M. K., Weitkamp, E. A., Sage, A. M., Grieshop, A. P., Lane, T. E., Pierce, J. R. and Pandis, S. N.: Rethinking organic aerosols: semivolatile emissions and photochemical aging. Science, 315, 1259-62, 2007.

Atkinson, R. W., Fuller, G. W., Anderson, H. R., Harrison, R. M. and Armstrong, B.: Urban ambient particle metrics and health: a time-series analysis, Epidemiology, 21, 501-511, 2010.

Biswas, S., Ntziachristos, L., Moore, K. F. and Sioutas, C: Particle volatility in the vicinity of a freeway with heavy-duty diesel traffic, Atmos. Environ., 41, 3479-3493, 2007.

Chan, A. W. H., Isaacman, G., Wilson, K. R., Worton, D. R., Ruehl, C. R., Nah, T., Gentner, D. R., Dallmann, T. R., Kirchstetter, T. W., Harley, R. A., Gilman, J. B., Kuster, W. C., de Gouw, J. A., Offenberg, J. H., Kleindienst, T. E., Lin, Y. H., Rubitschun, C. L., Surratt, J. D., Hayes, P. L., Jimenez, J. L. and Goldstein, A. H.: Detailed chemical characterization of unresolved complex mixtures in atmospheric organics:insights into emission sources, atmospheric processing, and

secondary organic aerosol formation, J. Geophys. Res.:Atmospheres, 118, 6783-6796, 2013.

Chickos, J. and Lipkind, D.: Hypothetical thermodynamic properties: vapour pressures and vaporization enthalpies of the even n-Alkanes from C78 to C92 at T= 298.15K by correlation-gas chromatography, J. Chem. Eng. Data, 53, 2432-2440, 2008.

Compernolle, S., Ceulemans, K. and Muller, J. -F.: Evaporation: a new vapour pressure estimation method for organic molecules including non-additivity and intramolecular interactions, Atmos. Chem. Phys., 11, 9431-9450, 2011.

Dall'Osto, M., Thorpe, A., Beddows, D.C.S., Harrison, R.M., Barlow, J.F., Dunbar, T., Williams, P.I. and Coe, H.: Remarkable dynamics of nanoparticles in the urban atmosphere, Atmos. Chem. Phys., 11, 6623-6637, 2011.

Donahue, N. M., Robinson, A. L., Stanier, C. O., and Pandis, S. N.: Coupled partitioning, dilution, and chemical aging of semivolatile organics, Environ. Sci. Technol., 40, 2635–2643, 2006.

Grieshop, A., Miracolo, M., Donahue, N., and Robinson, A.: Constraining the volatility distribution and gas-particle partitioning of combustion aerosols using isothermal dilution and thermodenuder measurements., Environ. Sci. Technol., 43, 4750, 2009.

Harrad, S., Hassoun, S., Callen Romero, M.S. and Harrison, R.M.: Characterisation and source attribution of the semi-volatile organic content of atmospheric particles and associate vapour phase in Birmingham, UK, Atmos. Environ., 37, 4985-4991, 2003.

Harrison, R. M., Beddows, D. S. and Dall'Osto, M.: PMF analysis of wide-range particle size spectra collected on a major highway, Environ. Sci. Technol., 45, 5522-5528, 2011.

Harrison, R. M., Dall'Osto, M., Beddows, D. C. S., Thorpe, A. J., Bloss, W. J., Allan, J. D., Coe, H., Dorsey, J. R., Gallagher, M., Martin, C., Whitehead, J., Williams, P. I., Jones, R. L., Langridge, J. M., Benton, A. K., Ball, S. M., Langford, B., Hewitt, C. N., Davison, B., Martin, D., Petersson, K. F., Henshaw, S. J., White, I. R., Shallcross, D. E., Barlow, J. F., Dunbar, T., Davies, F., Nemitz, E., Phillips, G. J., Helfter, C., Di Marco C. F. and Smith, S.: Atmospheric chemistry and physics in the atmosphere of a developed megacity (London): an overview of the REPARTEE experiment and its conclusions, Atmos. Chem. Phys., 12, 3065-3114, 2012.

Harrison, R.M., Jones, A.M., Beddows, D.C.S., Dall'Osto M. and Nikolova, I.: Evaporation of traffic-generated nanoparticles during advection from source, Atmos. Environ., 125, 1-7, 2016.

Joback, K. and Reid, R.: Estimation of Pure-component properties from group-contributions, Chem. Eng. Commun., 57, 233-243, 1987.

Jacobson, M.Z.: Development and application of a new air pollution modeling system. 2. Aerosol module structure and design, Atmos. Environ., 31, 131-144, 1997.

Jacobson, M. Z., Kittelson, D. B., and Watts, W. F.: Enhanced coagulation due to evaporation and its effect on nanoparticle evolution, Environ. Sci. Technol., 39, 9486- 9492, 2005.

Julin, J., Winkler, P. M., Donahue, N. M., Wagner, P. E. and Riipinen, I.: Nera-unity mass accomodation coefficient of organic molecules of varying structure, Environ. Sci. Technol., 48, 12083-12089, 2014.

Karl, M., Kukkonen, J., Keuken, M. P., Lützenkirchen, S., Pirjola, L., and Hussein, T.: Modeling and measurements of urban aerosol processes on the neighborhood scale in Rotterdam, Oslo and Helsinki, Atmos. Chem. Phys., 16, 4817-4835, doi:10.5194/acp16-4817-2016, 2016.

Karnezi, E., Riipinen, I. and Pandis, S. N.: Measuring the atmospheric organic aerosol volatility distribution: a theoretical analysis, Atmos. Meas. Tech. Discuss., 7, 2953-2965, 2014.

Kumar, P., Morawska, L., Birmili, W., Paasonen, P., Hu, M., Kulmala, M., Harrison, R. M., Norford, L. and Britter, R.: Ultrafine particles in cities, Environ. Intl., 66, 1-10, 2014.

Lemmon, E. W. and Goodwin, A. R. H.: Critical properties and vapour pressure equation for alkanes CnH2n+2: normal alkanes with $n \leq 36$ and isomers for n = 4 through n = 9, J. Phys. Chem. Ref. Data, 29, 1-39, 2000.

Li, R., Ning, Z., Majumdar, R., Cui, J., Takabe, W., Jen, N., Sioutas, C. and Hsiai, T.: Ultrafine particles from diesel vehicle emissions at different driving cycles induce differential vascular pro-inflamatory responses: implications of chemical components and NF-kB signaling, Part. Fibre Toxicol., 7-6, 2010.

May, A. A., Presto, A. A., Hennigan, C. J., Nguyen, N. T., Gordon, T. D., and Robinson, A. L.: Gas-particle partitioning of primary organic aerosol emissions: (2) Diesel vehicles, Environ. Sci. Technol., 47, 8288-8296, 2013.

Myrdal, P. B. and Yalkowsky, S. H.: Estimating pure component vapor pressures of complex organic molecules, Ind. Eng. Chem. Res., 36, 2494-2499, 1997.

Nannoolal, Y., Rarey, J., Ramjugernath, D. and Cordes, W.: Estimation of pure component properties: Part 1. Estimation of the normal boiling point of non-electrolyte organic compounds via
group contributions and group interactions, Fluid Phase Equilibr., 226, 45-63, 2004.

Nannoolal, Y., Rarey, J. and Ramjugernath, D.: Estimation of pure component properties: Part 3. Estimation of the vapor pressure of non-electrolyte organic compounds via group contributions and group interactions, Fluid Phase Equilibr., 269, 117-133, 2008.

Nikolova, I., Janssen S., Vos, P., Vrancken, K., Mishra, V. and Berghmans, P.: Dispersion modelling of traffic induced ultrafine particles in a street canyon in Antwerp, Belgium and comparison with observations, Sci. Total Environ., 412-413, 336-43, 2011.

Nikolova, I., MacKenzie, A. R., Cai, X., Alam, M. S. and Harrison, R. M.: Modelling component evaporation and coposition change of traffic-induced ultrafine particles during travel from street canyon to urban background, Faraday Discuss.,189, 529-546, 2016.

Pugh, T. A. M., MacKenzie, A. R., Whyatt, J. D. and Hewitt, C. N.: Effectiveness of green infrastructure for improvement of air quality in urban street canyons, Environ. Sci. Technol., 46, 7692-7699, 2012.

Robinson,. A. L., Donahue, N. M., Shrivastava, M. K., Weitkamp, E. A., Sage, A. M., Grieshop, A. P., Lane, T. E., Pierce, J. R. and Pandis, S. N.: Rethinking organic aerosols: semivolatile emissions and photochemical aging, Science, 315, 1259-1262, 2007.

Ronkko, T., Lahde, T., Heikkila, J., Pirjola, L., Bauschke, U., Arnold, F., Schager, H., Rothe, D., Yli-Ojanpera, J. and Keskinen, J.: Effects of Gaseous Sulphuric Acid on Diesel Exhaust Nanoparticle Formation and Characteristics, Environ. Sci. Technol., 47, 11882-11889, 2013.

Stein, S. E. and Brown, R. L.: Estimation of normal boiling points from group contributions, J. Chem. Inf. Comp. Sci., 34, 581-58, 1994.

Topping, D., Barley, M., Bane, M. K., Higham, N., Aumont, B., Dingle, N., and McFiggans, G.:

UManSysProp v1.0: an online and open-source facility for molecular property prediction and atmospheric aerosol calculations, Geosci. Model Dev.., 9, 899-914, 2016.

US EPA: Estimation Programs Interface Suite™ for Microsoft® Windows, v 4.11, United States Environmental Protection Agency, Washington, DC, USA, 2017.

Wehner, B., Philippin, S., Wiedensohler, A., Scheer, V. and Vogt, R.: Variability of non-volatile fractions of atmospheric aerosol particles with traffic influence, Atmos. Environ., 38, 6081-6090, 2004.

Xia, M., Viera-Hutchins, L., Garcia-Lloret, M., Rivas, M. N., Wise, P., McGhee, S. A., Chatila, Z. K., Daher, N., Sioutas, C. and Chatila, T. A.: Vehicular exhaust particles promote allergic airway inflammation through an aryl hydrocarbon receptor-notch signaling cascade, J. Allergy Clin. Immun., 136, 441-453, 2015.

TABLE LEGENDS

Table 1. Total mass M (ng m^{-3}) of nucleation mode peak particles at 1 s and 100 s of simulation for modal compositions $C_{16}H_{34}$-$C_{32}H_{66}$ and composition standard deviations, sigma. For comparison, the initial mass of the non-volatile material in the nucleation mode peak particles is 2.9 ng m^{-3}.

Table 2. Modal composition ranges and composition standard deviations, sigma, producing model results that approximate REPARTEE-like behaviour (see main text), for different vapour pressure parameterisations. Initial non-volatile core in the nucleation mode is set to 1%.

Table 3. Modal composition range and composition standard deviations, sigma, producing more realistic results that approximate REPARTEE-like behaviour. Vapour pressure

parameterisation follows Myrdal and Yalkowski (1997; B-c in Figure 3), Compernolle et al. (2011; Co in Figure 3), and Nannoolal 2008; A-a in Figure 3). Column 'cn' indicates the carbon number of compounds n in the modal composition with a contribution bigger than 1%.

FIGURE LEGENDS

Figure 1. A GC×GC chromatogram (contour plot) indicating homologous series of compounds identified in diesel engine exhaust emissions. Emissions from a light-duty diesel engine operating at 1800 revolutions per minute and 1.4 bar brake mean effective pressure. Compounds identified in the contour plot are indicated by the coloured polygons – Lower black polygons are n- + i-alkanes; red polygons are monocyclic alkanes; green polygons are bicyclic alkanes; pink polygons are aldehydes + ketones; and upper black polygons are monocyclic aromatics. Each peak in the contour plot represents a compound present in the emissions; warmer colours (e.g. red) are more intense peaks while colder colours (blue) are smaller peaks. Contour plot were produced by GC Image v2.5. Bar charts above show the volatility distribution of total alkanes (red) and total identified species (black), indicating that the majority of the emissions consist of alkanes. For details of the compound attribution method, see Alam et al. (2017).

Figure 2. An example of nucleation mode UFP compositions, represented as mass fractions for surrogate compounds $C_nH_{(2n+2)}$, n = [16:32], and described by a Gaussian distribution centred on $C_{24}H_{50}$ with standard deviation, σ, from 1 to 5.

Figure 3. Vapour pressure data for selected n-alkanes $C_nH_{(2n+2)}$ where n =[16:32] at 298K. Abbreviations in the legend point to the source as follows: A and B refer to the vapour pressure data from Nannoolal et al. (2008) and Myrdal and

Yalkowsky (1997), respectively; -a, -b and -c refer to the boiling point of Joback and Reid (1987), Stein and Brown (1994) and Nannoolal et al. (2004), respectively; ES refers to Epi Suite calculator (U.S. Environmental Protection Agency); Co to Compernolle et al. (2011); Ch to Chickos and Lipkind (2008), LG to Lemmon and Goodwin (2000).

Figure 4. Nucleation mode peak diameter Dp [nm] at 1 s of simulation depending on the modal composition and the composition standard deviation. The initial nucleation mode peak diameter is at 23nm (not shown on the figure).Vapour pressure data follows Compernolle et al. (2011).

Figure 5. Nucleation mode peak diameter Dp [nm] at 100 s of simulation depending on the modal composition and the composition standard deviation. The initial nucleation mode peak diameter is at 23nm (not shown on the figure).Vapour pressure data follows Compernolle et al. (2011).

Figure 6. $D_{pg,nuc}$ difference between the nucleation mode peak diameter (nm) when using B-c vapour pressure and the nucleation mode peak diameter when using A-a vapour pressure for modal compositions $C_nH_{(2n+2)}$ where n = [16:32].

Figure 7. Nucleation mode peak diameter Dp [nm] at 100 s: the '100-s effective non-volatile core' for the nucleation mode. Results are shown at 1%, 5% and 10% initial non-volatile material in the nucleation mode particles, modal composition $C_{16}H_{34}$ and for various composition standard deviations.

1s Centre @ Sigma	$C_{16}H_{34}$	$C_{17}H_{36}$	$C_{18}H_{38}$	$C_{19}H_{40}$	$C_{20}H_{42}$	$C_{21}H_{44}$	$C_{22}H_{46}$	$C_{23}H_{48}$	$C_{24}H_{50}$	$C_{25}H_{52}$	$C_{26}H_{54}$	$C_{27}H_{56}$	$C_{28}H_{58}$	$C_{29}H_{60}$	$C_{30}H_{62}$	$C_{31}H_{64}$	$C_{32}H_{66}$
1	2.9	2.9	2.9	2.9	7.4	23.6	38.1	46.8	51.0	52.6	53.2	53.4	53.4	53.5	53.5	53.5	53.5
2	2.9	2.9	3.2	6.9	14.3	24.1	34.0	42.1	47.0	50.3	52.1	52.9	53.3	53.4	53.4	53.5	53.5
3	3.7	5.4	8.4	12.9	18.5	24.9	31.6	38.1	43.5	46.8	49.3	51.0	52.1	52.8	53.1	53.3	53.4
4	8.0	10.6	13.7	17.6	21.8	26.4	31.0	35.4	39.7	43.7	46.2	48.2	49.8	50.9	51.8	52.3	52.7
5	12.8	15.3	18.1	21.1	24.4	27.7	31.2	34.4	37.6	40.2	43.0	45.4	47.0	48.4	49.5	50.4	51.2
100s Centre @ Sigma																	
1	2.9	2.9	2.9	2.9	2.9	2.9	2.9	2.9	6.1	23.8	38.9	47.5	51.3	52.8	53.3	53.5	53.6
2	2.9	2.9	2.9	2.9	2.9	2.9	3.0	6.2	14.3	24.8	34.8	42.5	47.6	50.6	52.1	52.9	53.2
3	2.9	2.9	2.9	2.9	3.1	4.2	7.1	11.9	18.2	25.2	31.9	37.8	42.6	46.1	48.6	50.3	51.4
4	2.9	3.0	3.3	4.1	5.6	7.9	11.1	15.1	19.7	24.6	29.3	33.8	37.7	41.1	43.8	46.1	47.8
5	3.7	4.4	5.4	6.9	8.7	11.1	13.8	17.0	20.2	23.7	27.2	30.6	33.7	36.6	39.2	41.4	43.4

Table 1. Total mass M (ng m^{-3}) of nucleation mode peak particles at 1 s and 100 s of simulation for modal compositions $C_{16}H_{34}$-$C_{32}H_{66}$ and composition standard deviations, sigma. For comparison, the initial mass of the non-volatile material in the nucleation mode peak particles is 2.9 ng m^{-3}.

Vapour pressure Sigma	B-c	Co	A-a
1	<= $C_{25}H_{52}$	<= $C_{23}H_{48}$	<= $C_{20}H_{42}$
2	<= $C_{24}H_{50}$	<= $C_{22}H_{46}$	<= $C_{19}H_{40}$
3	<= $C_{23}H_{48}$	<= $C_{21}H_{44}$	<= $C_{17}H_{36}$
4	<= $C_{21}H_{44}$	<= $C_{19}H_{40}$	-
5	<= $C_{20}H_{42}$	<= $C_{17}H_{36}$	-

Table 2. Modal composition ranges and composition standard deviations, sigma, producing model results that approximate REPARTEE-like behaviour (see main text), for different vapour pressure parameterisations. Initial non-volatile core in the nucleation mode is set to 1%.

Vapour pressure Sigma	B-c	Co	A-a	cn -/+
1	-	-	-	2
2	$C_{21}H_{44}$-$C_{24}H_{50}$	$C_{21}H_{44}$-$C_{22}H_{46}$	-	4
3	$C_{19}H_{40}$-$C_{23}H_{48}$	$C_{19}H_{40}$-$C_{21}H_{44}$	-	7
4	<= $C_{21}H_{44}$	<= $C_{19}H_{40}$	-	9
5	<= $C_{20}H_{42}$	<= $C_{17}H_{36}$	-	11

Table 3. Modal composition range and composition standard deviations, sigma, producing more realistic results that approximate REPARTEE-like behaviour. Vapour pressure parameterisation follows Myrdal and Yalkowski (1997; B-c in Figure 3), Compernolle et al. (2011; Co in Figure 3), and Nannoolal et al., 2008; A-a in Figure 3). Column 'cn' indicates the carbon number of compounds n in the modal composition with a contribution bigger than 1%.

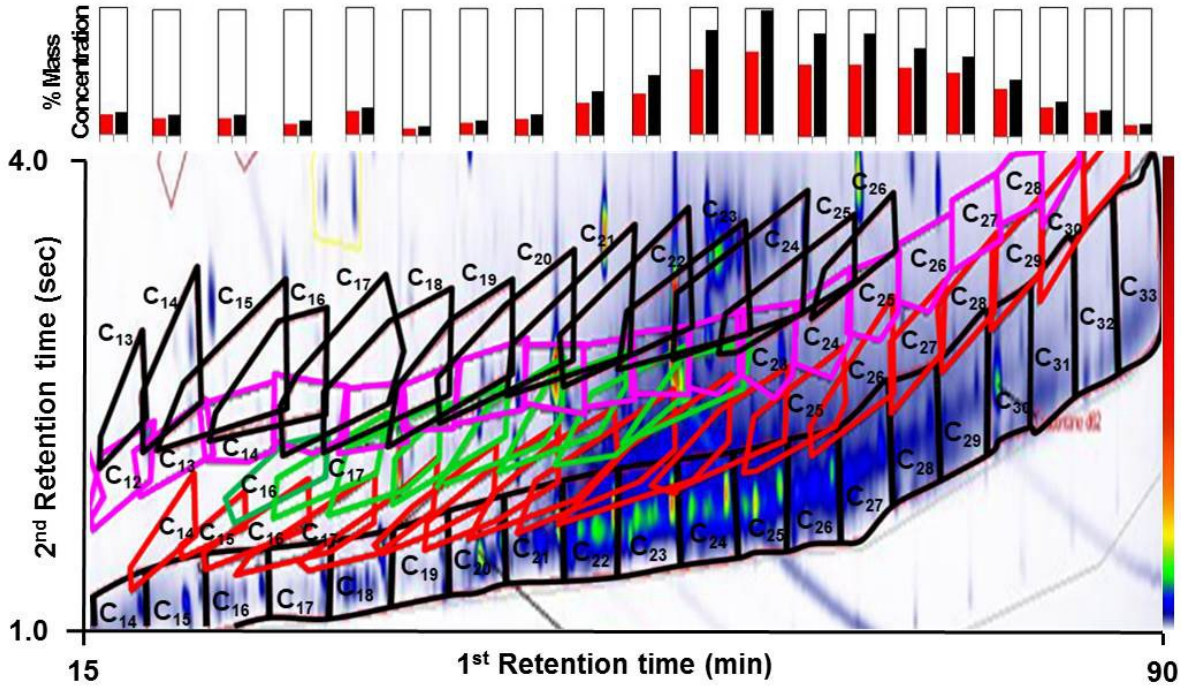

Figure 1. A GC×GC chromatogram (bottom panel, contour plot) indicating homologous series of compounds identified in diesel engine exhaust emissions. Emissions from a light-duty diesel engine operating at 1800 revolutions per minute and 1.4 bar brake mean effective pressure. Compounds identified in the contour plot are indicated by the coloured polygons – Lower black polygons are n- + i-alkanes; red polygons are monocyclic alkanes; green polygons are bicyclic

alkanes; pink polygons are aldehydes + ketones; and upper black polygons are monocyclic aromatics. Each peak in the contour plot represents a compound present in the emissions; warmer colours (e.g. red) are more intense peaks while colder colours (blue) are smaller peaks. Contour plot were produced by GC Image v2.5. Bar chart (top panel) show the volatility distribution of total alkanes (red) and total identified species (black), indicating that the majority of the emissions consist of alkanes. For details of the compound attribution method, see Alam et al. (2017).

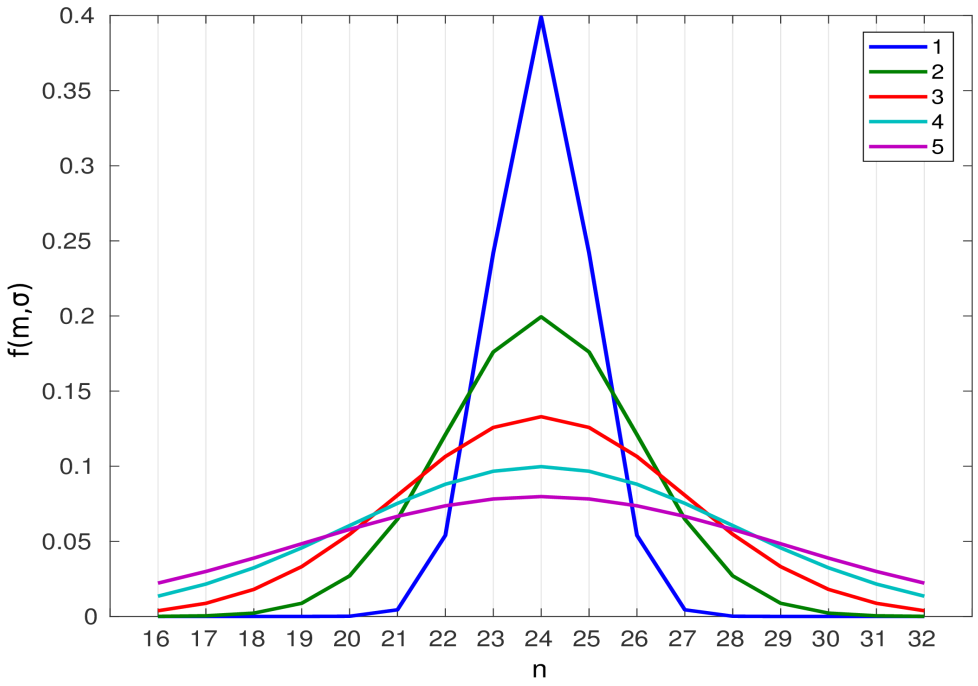

Figure 2. An example of nucleation mode UFP compositions, represented as mass fractions for surrogate compounds $C_nH_{(2n+2)}$, n = [16:32], and described by a Gaussian distribution centred on $C_{24}H_{50}$ with standard deviation, σ, from 1 to 5.

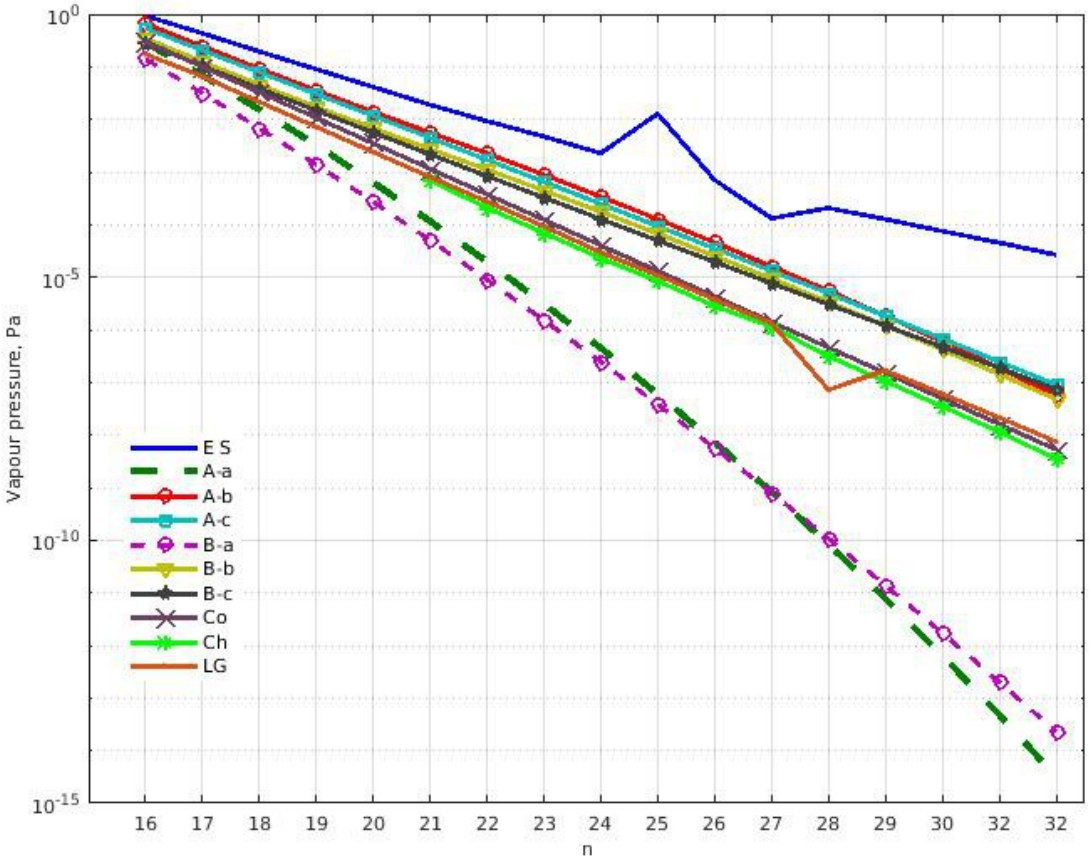
Vapour pressure, Pa
10^{0}
10^{-5}
10^{-10}
10^{-15}
16 17 18 19 20 21 22 23 24 25 26 27 28 29 30 32 32
n
E S
A-a
A-b
A-c
B-a
B-b
B-c
Co
Ch
LG

Figure 3. Vapour pressure data for selected n-alkanes $C_nH_{(2n+2)}$ where n =[16:32] at 298K. Abbreviations in the legend point to the source as follows: A and B refer to the vapour pressure data from Nannoolal et al. (2008) and Myrdal and Yalkowsky (1997), respectively; -a, -b and -c refer to the boiling point of Joback and Reid (1987), Stein and Brown (1994) and Nannoolal et al. (2004), respectively; ES refers to Epi Suite calculator (U.S. Environmental Protection Agency); Co to Compernolle et al. (2011); Ch to Chickos and Lipkind (2008); LG to Lemmon and Goodwin (2000).

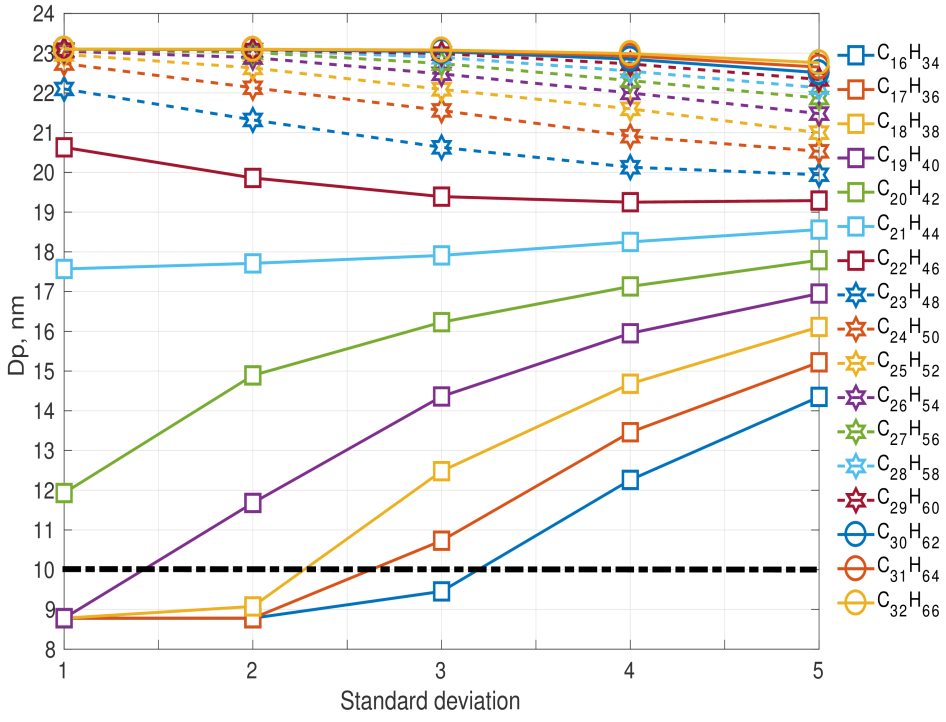

Figure 4. Nucleation mode peak diameter Dp [nm] at 1 s of simulation depending on the modal composition and the composition standard deviation. The initial nucleation mode peak diameter is at 23nm (not shown on the figure).Vapour pressure data follows Compernolle et al. (2011).

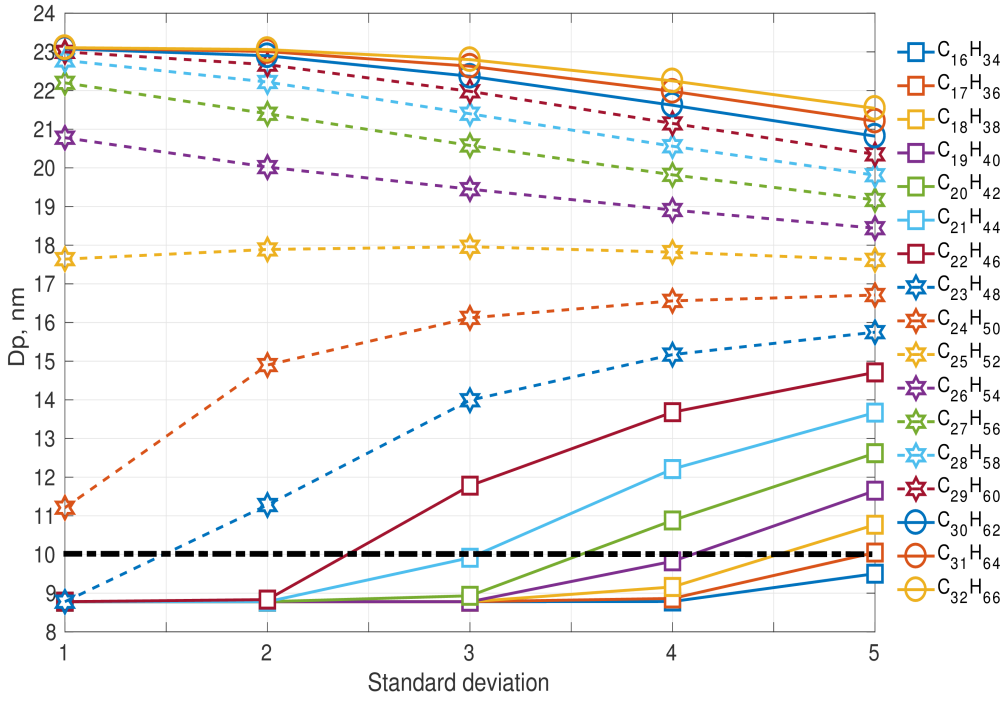

Figure 5. Nucleation mode peak diameter Dp [nm] at 100 s of simulation depending on the modal composition and the composition standard deviation. The initial nucleation mode peak

diameter is at 23nm (not shown on the figure).Vapour pressure data follows Compernolle et al. (2011).

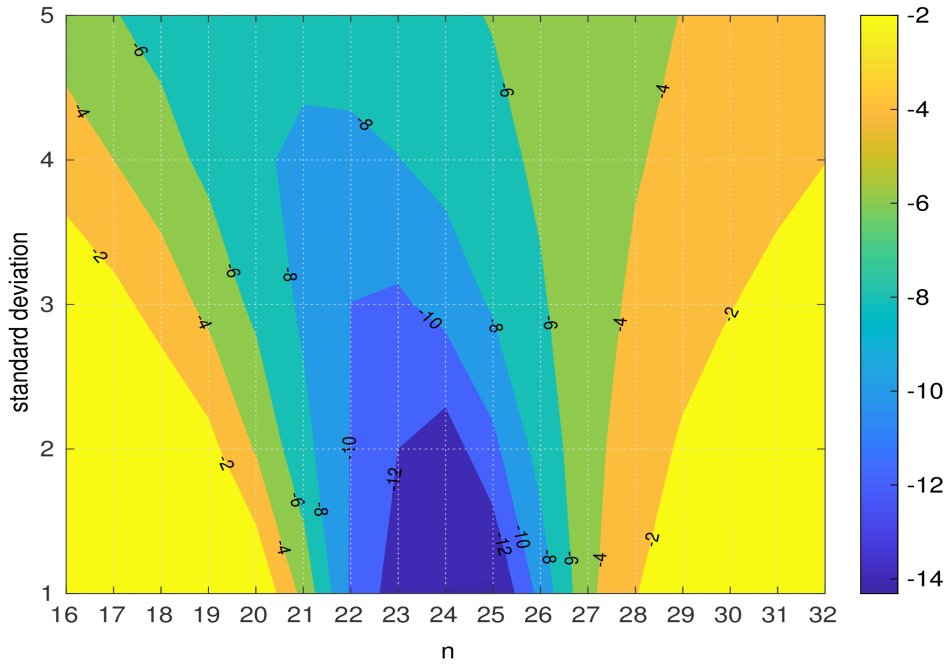

Figure 6. $D_{pg,nuc}$ difference between the nucleation mode peak diameter (nm) when using B-c vapour pressure and the nucleation mode peak diameter when using A-a vapour pressure for modal compositions $C_nH_{(2n+2)}$ where n = [16:32].

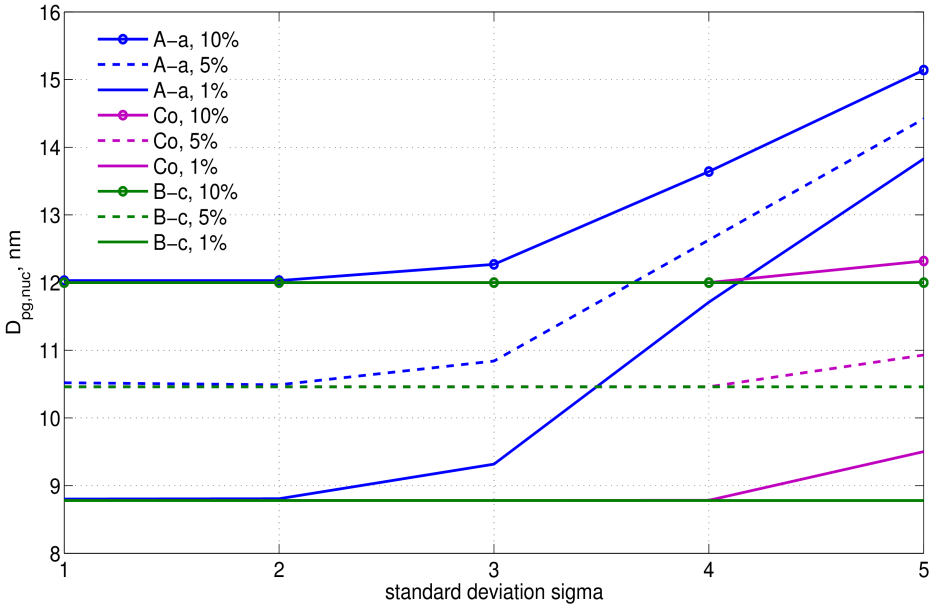

Figure 7. Nucleation mode peak diameter Dp [nm] at 100 s: the '100-s effective non-volatile core' for the nucleation mode. Results are shown at 1%, 5% and 10% initial non-volatile material in the nucleation mode particles, modal composition $C_{16}H_{34}$ and for various composition standard deviations.